Nano- and Microstructuring of SiO_2 and Sapphire with Fs-laser Induced Selective Etching

Maren Hörstmann-Jungemann, Jens Gottmann and Dirk Wortmann

Lehrstuhl für Lasertechnik, RWTH Aachen University, Steinbachstr. 15, 52074 Aachen, Germany
E-mail: maren.hoerstmann-jungemann@llt.rwth-aachen.de

Sub wavelength ripples perpendicular to the polarisation of the laser radiation are obtained by scanning a tightly focused beam (~1µm) of femtosecond laser radiation over the surface and through the volume of various materials. The ripple patterns extend coherently over many overlapping laser pulses and scanning tracks. The cross-sections and the surface of the ripples and in volume nanoplanes are investigated using electron microscopy. By using microscope objectives with higher Numerical Apertures micro-channels can be fabricated with a technique called In Volume Selective Laser Etching (ISLE).

DOI: 10.2961/jlmn.2009.02.0011

Keywords: ripple, nanoplanes, LIPPS, femtosecond, ultra short pulsed laser

1. Introduction

Ripples or, in general, laser-induced periodic surface structures (LIPSS) have been observed substantially near the ablation threshold by many authors since the beginning of laser ablation four decades ago [1]. The great variety of experimental LIPSS was subsumed into theoretical approaches [1-3]. In the most common type of surface topography, a periodicity of about the wavelength λ of the laser radiation is observed. This has been attributed to interference between the incident and scattered laser radiation or excited surface waves [5]. Smaller or broader spacing Λ between the ripples occurs if the laser radiation has an inclination θ to the surface normal. The dependence $\Lambda=\lambda/(1\pm\sin\theta)$ has been found, where the plus and the minus refer to the downwards and the upwards running surface wave on the inclined surface [2]. Ripple structures with sub-wavelength periodicity created by femtosecond laser pulses have been reported [12-14]. Sub-wavelength ripples formation is an increasing field of research for groups all over the world [15-21].

Because of the wide range of LIPSS, many other explanations have been considered [2, 6-8]. In most cases the ripple orientation is found to be perpendicular to the incident polarization.

Efforts were made to avoid ripples in micro structuring as their formation limits the precision of laser procession [4, 9, 10]. Otherwise it seems to be possible to utilize the ripples for micro and nano structuring [4], e.g. for the fabrication of gratings [11].

Reproducible sub-wavelength ripples are presented with periodicity from $\Lambda\approx\lambda/4$ to $3\times\lambda/4$ (110-600nm) [22] depending on the material properties and the applied wavelength. But unlike the classical ripple period the sub-wavelength ripple period can not be explained by the classical approach.

2. Experimental set up

The structured materials are fused silica and sapphire. The sample surface is polished to optical quality and cleaned in an ultrasonic bath of ethanol.

For the micromachining of the structures an Yb:glass fiber chirped pulse amplifier (FCPA IMRA µJewel D1000, λ=1045 nm, τ=500 fs, f=0.1-5 MHz, P_{av}=1.8 W) and a CPA-laser system (Thales Concerto λ=800 nm, τ=100 fs, f=1kHz) is used. The beam is linear polarized and the energy is adjusted using a half-wave plate and an additional polarizer. The sample is moved with a computer controlled positioning stage (Kugler Microstep). The three perpendicular translation axes provide an absolute accuracy of 100 nm, a repeatability of 250 nm and a maximum positioning speed of up to 2 mm/s (used positioning speed is 1mm/s). Several microscope objectives (20x/N.A.=0.4, 50x/N.A.=0.55, 100x/N.A.=0.95) are used for the fabrication of periodic structures. The applied pulse energy is adjusted to the fluence of the ablation threshold for each material. The ablation threshold is defined as the fluence where the first changes of the surface are detectable by optical microscopy. The samples are processed by scanning the focused laser radiation over the surface and through the volume. The scanning speed is chosen in the way that the pulse spacing d (distance between two successive pulses) is smaller than 10 nm (resulting in an overlap of at least 99%).

All experiments are performed in ambient air at normal incidence. For the comparison of laser-induced surface structures and in-volume structures the focus position is varied from 10 µm above to 100 µm below the surface. To investigate not only the surface but also the volume structures a cross-section polish is prepared. Afterwards the sample is cleaned in an ultrasonic bath of pure ethanol and investigated by scanning electron microscopy (SEM).

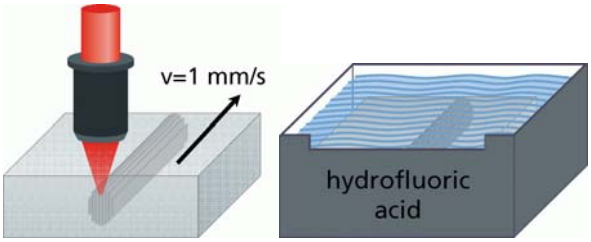

Fig. 1: ISLE (In volume selective laser etching): 1) Irradiation of the sample in the volume (left). 2) Etching of the irradiated sample in HF acid for 24 hrs (right).

For in-volume structuring of sapphire the beam is transferred into a microscope objective with N.A.=0.55 (0.8) and focused in a depth of 150 µm below the surface of the sample. The objective with N.A.=0.8 allows an adjustable compensation of the spherical aberrations for a depth between 0.1 and 1 mm in fused silica. The linear spot size is approximately 1 µm. To write adjacent lines the sample is moved by the three axes translation stage along the y-axis (propagation direction of the laser is along the z-axis). The used writing speed ranges from 0.1 to 1 mm/s (Fig. 1 (left)). Since the writing speed is significantly small compared to the repetition rate of the laser, the pulse to pulse overlap is large and the laser affected zones can be considered as lines along the scanning direction. The polarization of the laser beam is set parallel to the scanning direction. After irradiation, the samples are lapped from both sides (perpendicular to the scanning direction) to remove the irregular irradiated parts due to diffraction and reflection caused by the edges of the sample. Areas irradiated with less energy than the ablation threshold are not necessarily modified. For a better control of the etching process these areas are removed. Afterwards the sample is immersed in a 40% aqueous solution of HF acid for 24 hours (Fig. 1 (right)) and cleaned in an ultrasonic bath of ethanol.

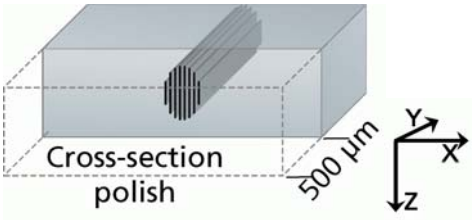

Fig. 2: ISLE 3) Preparation of a cross-section polish in different depth for SEM investigations.

After etching the end facets of the sample and by that the entrance of the etched micro channels are investigated by SEM. By lapping and polishing of the faces normal to the irradiated lines cross-sections of the periodic structures and micro-channels are produced in a depth from 100 to 1000 µm beneath the entrance of the etched areas (Fig. 2) to investigate the depths and shapes of the etched micro-channels.

3. Coherent continuation of sub-wavelength ripples

Ripple structures with spacing significantly smaller than the irradiation wavelength are observed on all samples. The direction of the resulting structures is perpendicular to the polarization of the laser radiation (Fig. 3).

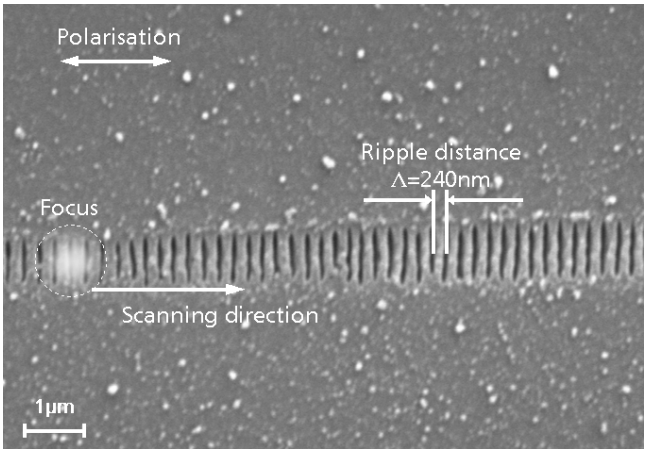

Fig. 3: Coherently continued ripples by scanning parallel to the polarization on the surface of fused silica (λ=800 nm, τ=100 fs, f=1 kHz, E_p=0.2 µJ, N.A.= 0.7).

Regardless to the scanning direction of the laser radiation the ripples continue coherently in respect to the polarization over many overlapping laser pulses [22]. Ripples can even be continued coherently in 2d by scanning several overlapping tracks (Fig. 4).

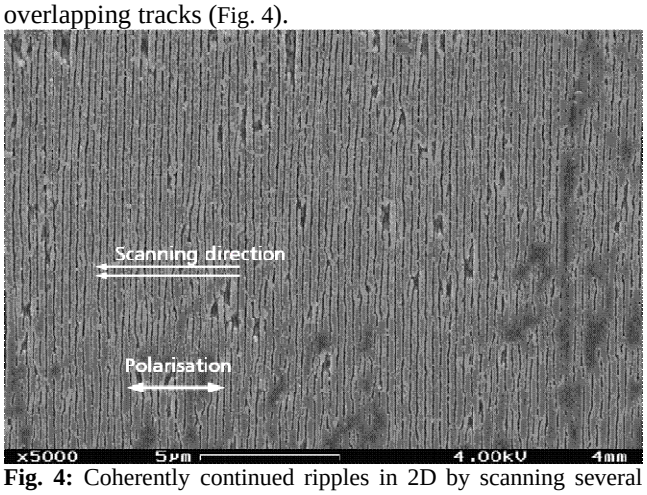

Fig. 4: Coherently continued ripples in 2D by scanning several tracks with an offset of 400 nm on the surface of fused silica (λ=800 nm, τ=100 fs, f=1 kHz, E_p=0.2 µJ, N.A.=0.7).

3.1 Cross-section of sub-wavelength ripples

The samples with sub-wavelength ripples are lapped and polished to investigate the cross-section by SEM. In fused silica the ripples consist of very thin (<50 nm) cracks or planes where the material density is reduced. They are up to 500-700 nm deep (Fig. 5).

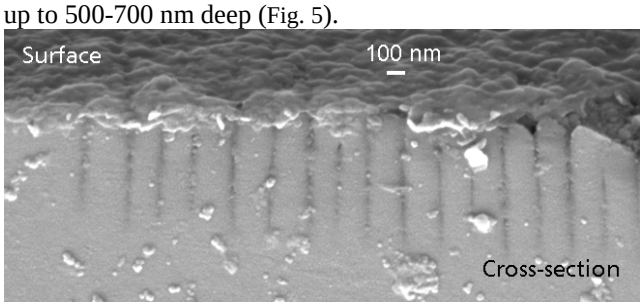

Fig. 5: Scanning electron micrographs of cross-section of surface ripples in fused silica (λ=1045 nm, τ=500 fs, f=3 MHz, N.A.=0.7).

The ripples are covered by a debris layer of ≈100nm thickness. The resulting ripple structure on the surface is

similar to the nanoplanes observed during the fs-laser induced modification in the volume of fused silica [26]. In Fig. 6 the changeover between ripples on the surface and nanoplanes in the volume of sapphire can be seen. Therefore the explanation of the formation of sub-wavelength ripples may also be applied as a model for the formation of nanoplanes in the volume.

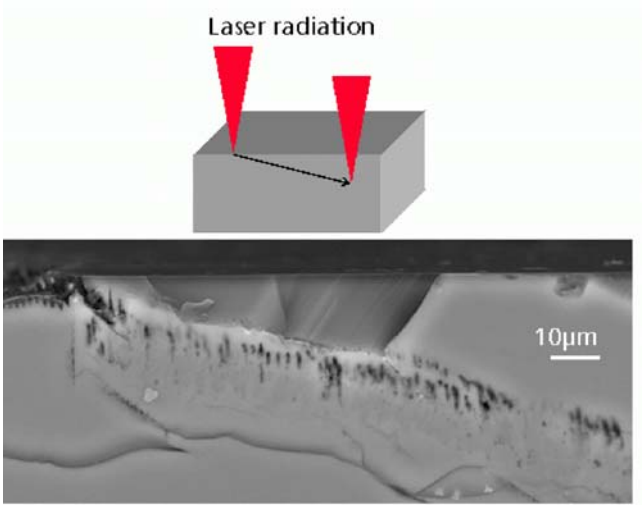

Fig. 6: Sketch of the laser irradiation method (top) and scanning electron micrograph of the cross-section of the ripples in the volume of sapphire along the laser irradiated track (bottom) (λ=1045 nm, τ=500 fs, f=3 MHz, N.A.=0.7).

In sapphire the ripples are saw-tooth like modifications with ≈100 nm width and ≈250 nm depth, covered by a 100-500 nm thick layer of modified sapphire and debris (Fig. 7 top).

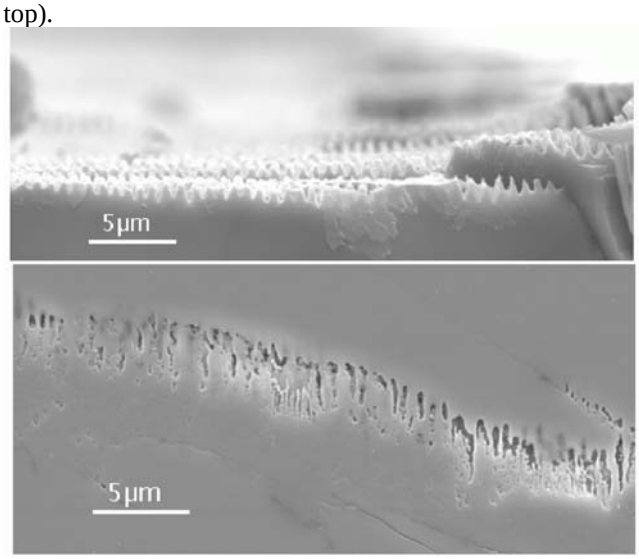

Fig. 7: Scanning electron micrograph of the cross-section of ripples in sapphire after cleaning and etching (λ=1045 nm, τ=500 fs, f=3 MHz, N.A.=0.7), focus at the surface (top) and below the surface in the volume (bottom).

The layer of modified sapphire and debris can be removed by chemical etching with an aqueous solution of HF acid (Fig. 7 top). The sapphire sample is immersed for 15min in a 40% HF acid, for a fused silica sample an etching time less then 10 min in 2-5% aqueous solution of HF acid is already enough.

By scanning the laser beam trough the volume of sapphire and fused silica structures very similar to the surface sub-wavelength ripples are observed in the volume (Fig. 6 bottom). The periodical structures in the volume are called nanoplanes [22]. Especially the period of the self organizing structures is identical. Because of this the fundamental mechanisms of the formation of periodic surface structures with sub-wavelength period on dielectrics and the formation of nanoplanes or nano-cracks in the volume of dielectrics are considered to be identical. The considered feedback mechanism leading to coherent periodic sub-wavelength structures is based on scattering of the laser radiation at the nanostructures, the excitation of plasmonic waves in the volume of the material, interference of the electrical fields and the resulting intensity modulation. Close to the surface this intensity fringes/ modulation may cause the localized ablation of the material, resulting in the formation of sub-wavelength ripples without subsequent etching. This is also an explanation of single isolated but well established ripples on the surface of sapphire and fused silica [24].

The period of the sub-wavelength ripples depend beside the wavelength on the material (fused silica (FS, a-SiO_2), Si, $LiNbO_3$, ZrO_2, Al_2O_3, MgF2, LiF, ZBLAN, Au, Cu and PTFE have been investigated [30]) and are sub-linear dependent on the wavelength of the used laser radiation. In this work the ripple period of Sapphire (Λ≈770 nm with λ=1045 nm) and fused silica (Λ≈240 nm with λ=800 nm) are measured. This reveals a dependency of the ripple period Λ on the wavelength λ of approximately 3λ/4 (sapphire) and λ/3 (fused silica). Therefore the transient dielectric function modified during and after the laser pulse has to be considered for the modeling of the period of the surface ripples and the in-volume nanoplanes.

4. Hollow nanoplanes and micro channels in sapphire

To produce hollow nanoplanes and micro channels in the volume of sapphire a technique called ISLE (In Volume Selective Laser Etching) is used.

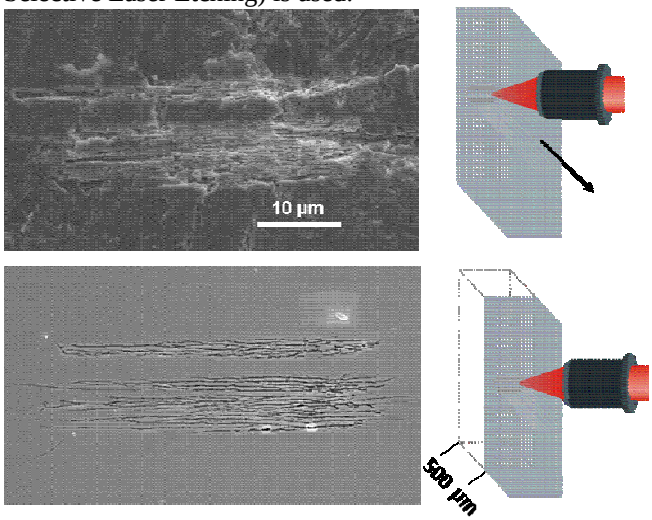

Fig. 8: SEM images of cross-sections of hollow nanoplanes in the entrance area (top) and in 500 µm depth in the volume (bottom) of sapphire, three parallel lines written with λ=1045 nm, f=500 kHz, P=180 mW, N.A.=0.55.

After cleaning and investigating the entrance area of the nanoplanes (Fig. 8 top) a cross section of the same sample in a depth of up to 500 µm is investigated (Fig. 8 bottom). SEM images of the surface rectangular to the scan direction make the different etch rates in the modified area and in the crystalline sapphire visible. The unmodified part is nearly not etched, therefore the surface only becomes rough during etching. At the entrance of the modified area etched structures (nanostructures) are visible. Structures with the same shape can be found in different depth from the entrance area (Fig. 8). The average width of the nanostructures is about 200 nm (x-direction), the distance is about 300 nm (x-direction), the length is about 40 µm (z-direction) and the depth is at least 500 µm (y-direction) without interruption and permeable for liquids (e.g. the aqueous solution of HF acid and the solvent). This leads to a aspect ratio (depth:width) of 2500.

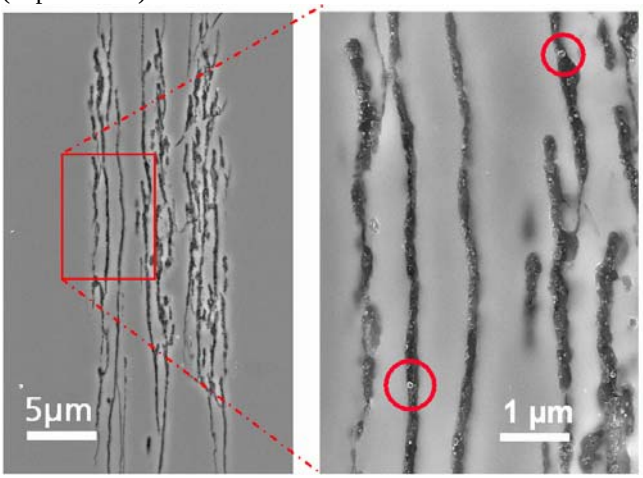

Fig. 9: SEM images of cross sections of hollow nanoplanes in 500µm depth in the volume of sapphire, three parallel lines written with λ=1045 nm, f=500 kHz, P=180 mW, N.A.=0.55.
(left and magnification right), Laser beam propagated from top to bottom The residue of the polishing suspension is marked with red circles (right).

The residue of the polishing suspension (≈30-50 nm sized spheres) is visible in the nanostructures (Fig. 9 right). This supply evidence that the nanoplanes are hollow during the fabrication of the cross-section polish.

We consider here the formations of nanoplanes like these structures are called by Hnatovsky and Yang [28, 29]. Compared to Hnatovsky our structures are not so well organized, perhaps due to the comparably high pulse duration (t=500 fs) which was used [28]. Nevertheless, in the here presented work, the hollow nanoplanes with a width of about 200 nm are etched in one step to a depth (y-direction) of at least 500 µm or more. This corresponds to an aspect ratio (depth : width) of more than 2500. Compared to the calculated Rayleigh length r_z=8 µm of the laser beam the modified and therefore etched region is elongated by a factor of more than 5 by spherical aberrations and by propagation effects (Fig. 9 left).

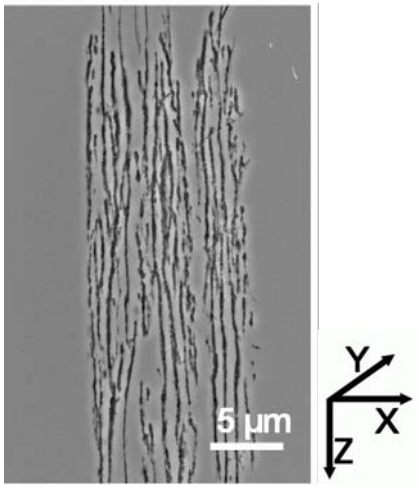

Fig. 10: SEM images of cross sections of hollow nanoplanes in 500µm depth in the volume of sapphire, three parallel lines written with λ=1045 nm, f=500 kHz, P=300 mW, N.A.=0.55. Higher energy leads to more dense structures.

Using higher pulse energies leads to an increase of the size of the modified area and an increasing number of hollow nanoplanes within it, while the width and the distance of the hollow nanoplanes stays the same (Fig. 10).

By using microscope objectives with a higher Numerical aperture or the possibility of spherical aberration correction hollow micro channels can be produced.

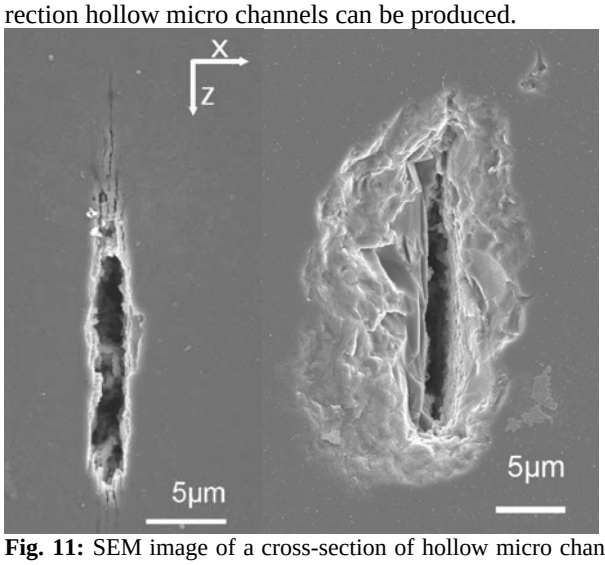

Fig. 11: SEM image of a cross-section of hollow micro channels produced with f=100 kHz, El=500 J/m, N.A.=0.7 (left) and N.A.=0.8 (right).

In Fig. 11 left the micro channel is produced with a N.A. of 0.7 instead of 0.55 like the hollow nanoplanes. Due to the larger intensity in the smaller focus area the non-linear absorption is higher. By this the material is better etched and hollow micro-channels result instead of hollow nanoplanes. That the same process is as well for the nanoplanes as for the micro channels responsible can be seen in the coexistence of both (Fig. 11 left). Using a microscope objective with a even higher N.A. (0.8) leads, because of the higher absorption, also to crack formation (Fig. 11).

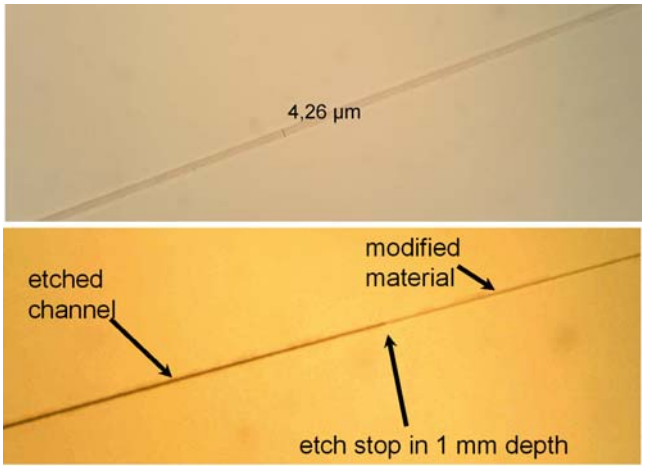

Fig. 12: Light microscope image of micro-channels in sapphire before etching (top) and after etching in 40% HF acid for 24h.

By investigating the sapphire sample with a transmitting light microscope the modified channel can already be seen before etching. The modified area is about 4 µm wide (Fig. 12 top). After immersion the etched and the not etched parts of the channel can be observed in the same way. This is the best way of measuring the channel length, whereas the diameter of the channel can be better defined with SEM images. After 24h etching in 40% HF acid the hollow micro-channel is about 1 mm (Fig. 12 bottom) long and has a diameter of 1.8 µm (Fig. 11 left). This reveals a aspect ratio (width: depth) of 550.

4.1 Second kind ripples

Because of the high shearing forces during the lapping and polishing process thin sheets of unmodified sapphire between the hollow nanoplanes sometimes break mechanically. This case allows investigating their surface.

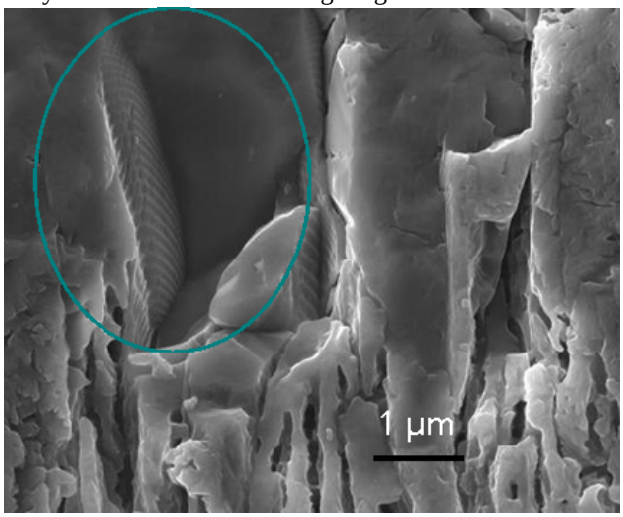

Fig. 13: SEM images of cross sections of hollow nanoplanes in 500 µm depth in the volume of sapphire: Sub-wavelength ripples parallel to the polarization on the surface of hollow nanoplanes, laser beam propagation from top to bottom.

On the surface of the hollow nanoplanes clean coherently sub-wavelength ripples with an orientation parallel to the electric field of the laser radiation are observed. The ripple period is about Λ=150 nm (Fig. 13). Because of their smaller period and their different orientation from sub-wavelength ripples known until now we call this structures second kind ripples. Similar sub wavelength ripples of a second kind oriented parallel to the laser radiation are occasionally observed on top of the sub-wavelength ripples on dielectric surfaces [24]. Therefore the fundamental mechanisms involved in the formation of sub-wavelength ripples and in-volume nanoplanes are considered to be identically.

Sometimes serial stings of hollow nano-channels (second kind ripples) with diameter ≈100 nm are observed among hollow nanoplanes (Fig. 14). These stings are considered as a superposition of nanoplanes parallel to the polarization with nanoplanes rectangular to the polarization of the electric field of the laser radiation.

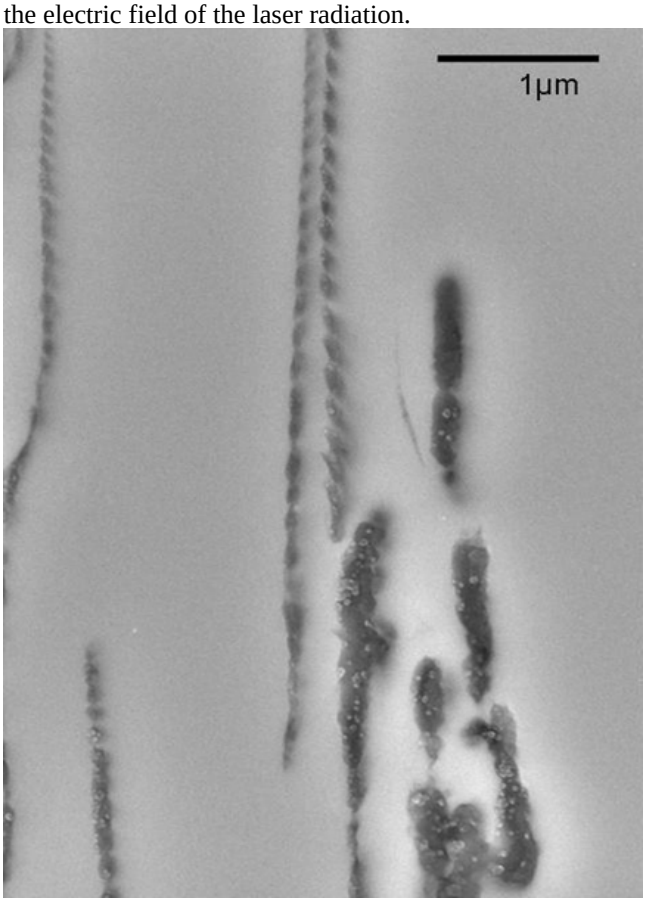

Fig. 14: SEM images of cross sections of hollow nano-channels (second kind ripples) between hollow nanoplanes in 500 µm depth in the volume of sapphire, laser beam propagation from top to bottom.

5. Conclusion

Sub-wavelength ripples on the surface of sapphire and fused silica continue coherently not only in one dimension but also in two dimensions on the surface by several scans with an offset. By investigating cross-sections of sub-wavelength surface ripples high aspect ratios (width: depth) larger then 10 in fused silica and about 2.5 in sapphire are observed. By scanning the laser radiation into the volume of sapphire and fused silica structures very similar to surface sub-wavelength ripples (hollow nanoplanes) are observed in the volume. Therefore the fundamental mechanisms of the formation of periodic surface structures with sub-wavelength period and the formation of nanoplanes or

nano-cracks in the volume of dielectrics are considered to be identical.

We have manufactured deep (up to 1 mm) micro-and nanostructures with sub-micrometer resolution in the volume of sapphire by femtosecond laser modification followed by chemical etching with aqueous solution of HF acid. The size and the shape of these structures can be controlled by varying the process parameters pulse energy, scan speed and N.A.. In either case a feature length of up to 1 mm (y-direction) and dimensions in the micrometer range (x-direction) resulting in an aspect ratio (depth: width) of up to 2500:1 for hollow nanoplanes and of up to 550:1 for hollow micro-channels.

On the surface of hollow nanoplanes in the volume of sapphire sub-wavelength ripples with a period of 150 nm are observed. Because of the orientation parallel to the electric field polarization of the laser radiation we call them second kind ripples.

Acknowledgments

The authors would like to thank IMRA America for the µJewel D-1000 laser system within the framework "Premier Application Lab" (PAL) at LLT RWTH Aachen University. The work on sub-wavelength ripples is funded by the German Research Foundation (DFG). We are grateful to our students Nelli Brandt and Martin Keggenhoff for a lot of work in the labs.

References

[1] M. Birnbaum, J. Appl. Phys. 36, 3688 (1965)
[2] Z. Guosheng, P. M. Fauchet, A. E. Siegman, Phys. Rev. B 26 (10) 5366 (1982)
[3] J. E. Sipe, J. F. Young, J. S. Preston, H. M. van Driel, Phys. Rev. B, 27 (2) 1141 (1983)
[4] A. Barborica, I. N. Milhailescu; V. S. Teodorescu, Phys. Rev. B, 49 (12), 8385 (1994)
[5] D. C. Emmony, R. P. Howson, L. J. Willis, Appl. Phys. Lett. 23 (11), 598 (1973)
[6] G. N. Maracas, G. L. Harris, C. A. Lee, R. A. McFarlane, Appl. Phys. Lett. 33(5) 453 (1978)
[7] N. R. Isenor, Appl. Phys. Lett. 31(3) 148 (1977)
[8] Y. F. Lu, W. K. Choi, Y. Aoyagi, A. Kinomura, K. Fujii, J. Appl. Phys. 80(12) 7052 (1996)
[9] M. Oron, G. Sørensen, Appl. Phys. Lett. 35(10) 782 (1979)
[10] P. Tosin, A. Blatter, W. Lüthy, J. of Appl. Phys. 78(6) 3797-3800 (1995)
[11] V. P. Aksenov, SPIE Vol 473 Symposium OPTIKA '84, p. 294 (1984)
[12] B. N. Chichkov, C. Momma, S. Nolte, F. von Alvensleben, A. Tünnermann, Phys. Rev. A 63, 109 (1996)
[13] D. Ashkenasi, A. Rosenfeld, H. Varel, M. Wähmer, E. E. B. Campbell, Appl. Surf. Sci. 120, 65-80 (1997)
[14] J. Bonse, S. Baudach, J. Krüger, W. Kautek, M. Lenzner, Appl. Phys. A 74 19-25 (2002)
[15] H. Varel, M. Wärmer, A. Rosenfeld, D. Ashkenasi, E. E. B. Campbell, Appl. Surf. Sci. 127-129, 128 (1998)
[16] A. M. Ozkan, A. P. Malshe, T. A. Railkar, W. D. Brown, M. D. Shirk, P. A. Molian, Appl. Phys. Lett. 75 (23), 3716 (1999)
[17] Q. Wu, Y. Ma, R. Fang, Y. Liao, Q. Yu, X. Chen, K. Wang, Appl. Phys. Lett. 82(11), 1703 (2003)
[18] A. Borowiec, H. K. Haugen, Appl. Phys. Lett. 82 (25) 4462 (2003)
[19] N. Yasumaru, K. Miyazaki, J. Kiuchi, Appl. Phys. A 76, 983 (2003)
[20] F. Costache, M. Henyk, J. Reif, Appl. Surf. Sci. 208-209, 486 (2003)
[21] P. Rudolph; W. Kautek, Thin Solid Films 453-454, 537-541 (2004)
[22] R. Wagner, J. Gottmann, Alexander Horn, Ernst W. Kreutz, Applied Surface Science 252, 8576-8579 (2006)
[23] R. Wagner, J. Gottmann, 8th international Conference on Laser Ablation 2005, Banff, Canada. J. Physics: Conference Series 59, 333 (2007)
[24] J. Gottmann, R. Wagner, PhotonicsWest 2006, Proc. of SPIE 6106, 61061R-42006, doi: 10.1117/12.644560, (2006)
[25] A. M. Streltsov, J. K. Ranka, A. L. Gaeta, Optics Letters 23 (10), 798 (1998)
[26] P.M. Fauchet, A.E. Siegman, J. Opt. Soc. Am. B 1 (3), 455-456 (1984)
[27] G. Schlaghecken, J. Gottmann, E. W. Kreutz, Reinhart Poprawe, Appl. Phys. A 79 (2004) 1255
[28] C. Hnatovsky, R.S. Taylor, E. Simova, P.P. Rajeev, D.M. Rayner, V.R. Bhardwaj, P.B. Corkum, Appl. Phys. A 84, 47-61 (2006)
[29] W. Yang, E. Bricci, P. Kazansky, J. Bovatsek, A. Arai, Opt. Express 14, 10117-10124 (2006)
[30] D.Puerto, W.Gawelda, J. Siegel, J. Bonse, G.Bachelier, J. Solis, Appl. Phys A, DOI 10.1007/s00339-008-4586-z (2008)

(Received: July 8, 2008, Accepted: June 5, 2009)